

MUON COLLIDER BASED ON GAMMA FACTORY, FCC-ee AND PLASMA TARGET *

J. Farmer, A. Latina, F. Zimmermann[†], CERN, Meyrin, Switzerland
A.P. Blondel, U. Geneva, Geneva, Switzerland
M. Antonelli, M. Boscolo, INFN-LNF, Frascati, Italy

Abstract

The LEMMA-type muon collider generates muon pairs by the annihilation of 45 GeV positrons with electrons at rest. Due to the small cross section, an extremely high rate of positrons is required, which could be achieved by a “Gamma factory” based on the LHC. Other challenges with the LEMMA-type muon production scheme include the emittance preservation of muons and muon-generating positrons upon multiple traversals through a target, and the merging of many separate muon bunchlets. These two challenges may potentially be overcome by (1) operating the FCC-ee booster with a barrier bucket and induction acceleration, so that all positrons of a production cycle are merged into one single superbunch, instead of storing $\sim 10,000$ separate bunches; and (2) sending the positron superbunch into a plasma target. During the passage of the positron superbunch, the electron density is enhanced more than 1000-fold without any increase in the density of nuclei, so that beamstrahlung and Coulomb scattering are essentially absent. We investigate prospects and difficulties of this approach, including emittance growth due to filamentation in the nonlinear plasma channel and due to positron self-modulation.

INTRODUCTION

The LEMMA scheme for a muon collider is based on the annihilation of positrons with electrons at rest [1]. The cross section for continuum muon pair production $e^+e^- \rightarrow \mu^+\mu^-$ has a maximum value of about $1 \mu\text{b}$ at a centre-of-mass energy of ~ 0.230 GeV, which corresponds to a e^+ beam energy of about 45 GeV, exactly as required for the FCC-ee operating at TeraZ factory and provided by the FCC-ee full-energy booster [2, 3].

MUON PRODUCTION BASED ON FCC-ee

Challenges with the LEMMA-type muon production scheme relate to the emittance preservation of muons and muon-generating positrons upon multiple traversals through a target, and the merging of many separate muon bunchlets, due to production by many separate e^+ bunches and numerous e^+ bunch passages [4].

These challenges may potentially be overcome by:

(1) Operating the FCC-ee booster with a barrier bucket and induction acceleration, so that all positrons of a cycle are merged into one single superbunch, instead of $\sim 10,000$ separate bunches.

(2) Sending the positron superbunch from the booster into a plasma target, where, during the passage of the e^+ superbunch, the electron density is enhanced more than 1000 fold without any significant density of nuclei, hence beamstrahlung and Coulomb scattering essentially absent.

POSITRON SUPERBUNCH

As described in the FCC-ee Conceptual Design Report [2], the FCC-ee booster can accelerate 3.5×10^{14} positrons every 50 s. Using the much more powerful Gamma Factory e^+ source, with a rate of $10^{16}\text{--}10^{17} e^+ s^{-1}$ [5], provided by laser excitation of partially stripped heavy-ion beams in the LHC or FCC-hh, and injecting into the booster during one or a few seconds, of order $10^{17} e^+$ can be accumulated, at the booster injection energy of ~ 20 GeV. The positrons can be captured into a single barrier RF bucket, with a final length of ~ 5 m, where the longitudinal density would be about 1000 times higher than the peak bunch density in the collider ring (without collision). The stability of this beam configuration would need to be examined, e.g., with regard to microwave and TMCI thresholds.

Accelerating the long superbunch containing $10^{17} e^+$ by 25 GeV requires a total energy of 0.4 GJ, or, if accelerated over 2 s, about 200 MW of RF power. This translates into an induction acceleration voltage of ~ 2 MV per turn, which is three orders of magnitude higher than the induction voltage of the KEK digital accelerator [6], but about 10 times lower than the induction RF voltage produced at the LANL DARHT-II [7], at much higher or lower repetition rate, respectively. On the ramp and at top energy, the full bunch length l_b can conceivably be compressed to the assumed $l_b \approx 5$ m, by squeezing the gap of the barrier bucket (which requires substantially more voltage for the barrier RF system) – also see [6, 8]. Tentative parameters of the e^+ superbunch are compiled in Table 1. We assume that the booster ring runs near the coupling resonance so that the emittance is shared between the two transverse planes. The matched beta function inside a plasma of e^- density n_e is estimated as $\beta_{x,y} \approx (\gamma/(2\pi n_e r_e))^{1/2}$. For a typical initial plasma e^- density of $n_e = 10^{23} \text{ m}^{-3}$, this leads to an initial matched beta of 7 mm, decreasing to 0.2 mm, as a result of e^- accumulation. The e^- oscillation wavelength $\lambda_p \approx \sqrt{2\pi/(r_e n_{e^+})}$ is $\sim 5 \mu\text{m}$.

PLASMA TARGET RESPONSE

As the 45 GeV e^+ beam enters the plasma, the plasma electrons will move to compensate the beam charge. However, the charge density of the e^+ beam is extremely high,

* Work supported by the European Union’s Horizon 2020 Research and Innovation programme under Grant Agreement No. 101004730 (iFAST).

[†] frank.zimmermann@cern.ch

Table 1: Tentative Parameters of the Positron Superbunch Sent Onto the Plasma Target

parameter	symbol	value	unit
beam energy	E_b	45	GeV
tot. bunch length	l_b	5	m
bunch population	N_b	1000	10^{14}
transv. rms emittance	$\varepsilon_{x,y}$	135	pm
init. β at plasma entrance	$\beta_{x,y}$	7	mm
init. rms beam size	$\sigma_{x,y}$	1.0	μm

initially 4×10^4 times the unperturbed plasma density. Neutralising this charge would require a cylinder of electrons at the unperturbed plasma density with a radius $\sim 250 \mu\text{m}$, far larger than the plasma skin depth.

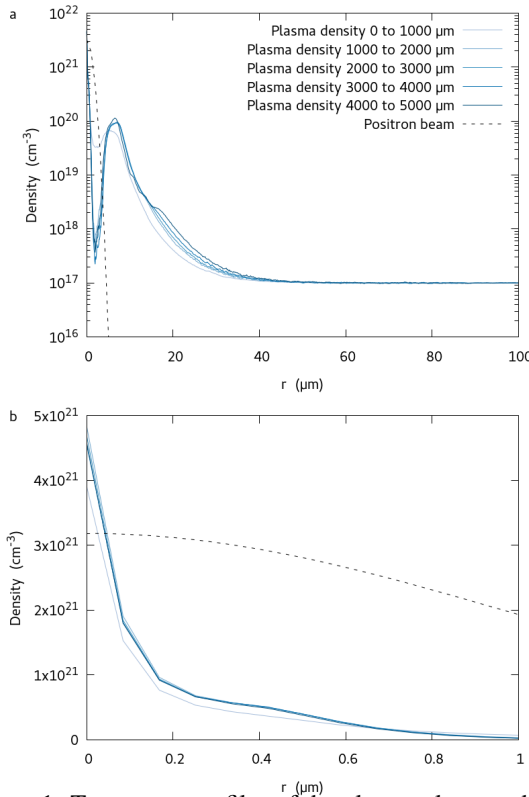


Figure 1: Transverse profiles of the plasma electron density as the positron bunch passes through the plasma, simulated with LCODE for the initial bunch distribution. The mean density over different distances behind the head of the beam are shown over a radial distance of up to $100 \mu\text{m}$ from the beam (a) and a zoom over $1 \mu\text{m}$ around the beam (b).

Simulations carried out with the 2D quasistatic particle-in-cell code LCODE [9–11] show that the electron density in the vicinity of the driver is greatly enhanced, as seen in Fig. 1 (a, top), allowing charge neutralisation over a radius of only $20 \mu\text{m}$. This enhancement of the plasma electron density is primarily due to the “return current” of the plasma electrons, which are dragged along by the beam. This mo-

tion causes the electrons to bunch together, increasing their density. Near the beam axis, shown in Fig. 1 (b, bottom), the electron density is further enhanced, up to $4 \times 10^{27} \text{m}^{-3}$, even exceeding the high central density of the positron beam. This occurs due to “trapping” of plasma electrons which oscillate transversely about the driver. This behaviour can be understood by considering the trajectories of a slice of plasma electrons as the drive beam passes through them, shown in Fig. 2. Particles at large radii oscillate about their equilibrium position, while particles at small radii reach the beam axis, resulting in oscillations about the driver. These oscillations are not ordered, and so particles can exchange energy, as in the Dawson sheet model of plasma wavebreaking [12]. This allows some fraction of particles to achieve large transverse momenta, resulting in their ejection from the plasma. Other particles, meanwhile, lose transverse momentum, becoming trapped in oscillations of smaller amplitude, leading to the high-density peak on the beam axis. This process of wavebreaking has been predicted for the AWAKE experiment [13] with an underdense proton driver [14]. We note that these simulations are extremely challenging due to the disparate scales involved, and further work is being carried out to verify full numerical convergence.

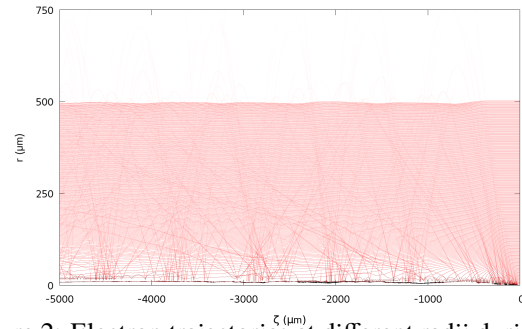


Figure 2: Electron trajectories at different radii during the passage of the positron bunch, simulated by LCODE.

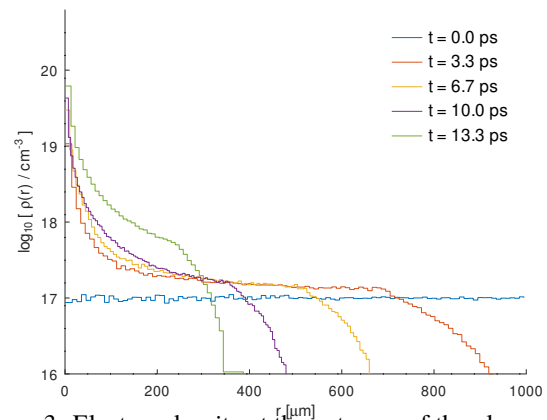


Figure 3: Electron density at the entrance of the plasma as a function of radial position for different time steps, simulated by RFTRACK, with only positron fields acting on electrons; during 3.3 ps the positron bunch advances by 1 mm.

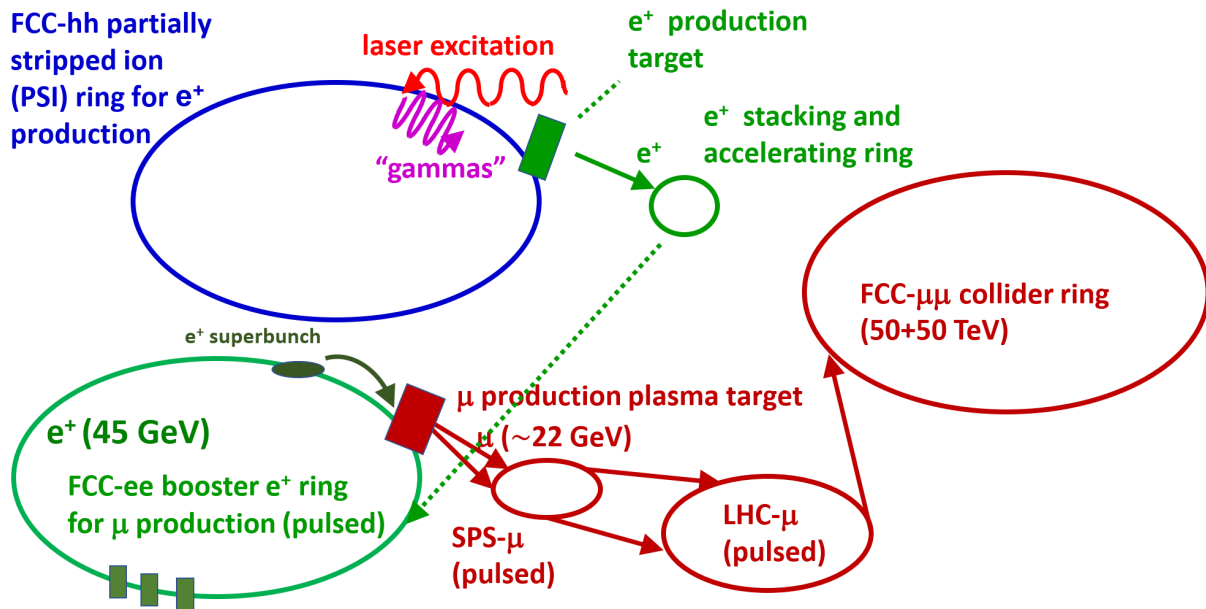


Figure 4: Concept of a 100 TeV μ collider based on FCC-hh and FCC-ee. In one of the FCC-hh rings, partially stripped heavy ions are collided with a pulsed laser to generate intense high-energy gamma rays that are converted into positrons, which are accumulated, then accelerated, and injected into a barrier bucket in the FCC-ee booster ring. The resulting superbunch is brought to a positron energy of 45 GeV, with induction acceleration, where the superbunch is extracted and sent into a hollow plasma channel, leading to a plasma electron density enhancement and, thereby, amplified annihilation into muon pairs. The muons are accelerated in a modified SPS and LHC, to be finally injected and accelerated in the second FCC-hh collider ring. This is a modified version of the scheme presented in Ref. [3].

While the code LCODE simulates the “steady-state” plasma response to the beam, another code, RFTRACK [15, 16], is presently being upgraded to model the edge effects as the beam enters the plasma, and to explore the resulting positron emittance growth. A preliminary result, with electrons experiencing only the fields of the positrons, is shown in Fig. 3, where the peak electron density, averaged on a coarser scale, reaches $n_e \approx 10^{26} \text{ m}^{-3}$ within 13.3 ps.

MUON PRODUCTION RATE

For the simulated plasma electron density $n_e \approx 4 \times 10^{27} \text{ m}^{-3}$, as in Fig. 1 (b, bottom), the positrons annihilate into muon pairs at a rate of $4 \times 10^{-7} \text{ m}^{-1}$.

Considering a 100 m long plasma channel yields $\sim 4 \times 10^{12}$ μ pairs per incident positron superbunch, with an initial muon energy of ~ 22 GeV (and an initial lifetime of 0.5 ms at this energy).

Overall, the described scheme, sketched in Fig. 4, would produce about 10^{12} muon pairs per cycle, with a cycle length of order 3 s. Even at an energy of 50 TeV, the muons would decay with a lifetime of only 1.1 s. This kind of cycle/lifetime ratio of about 3:1 might still be considered acceptable. On the other hand, for collision at 7 TeV muon beam energy in the existing LHC ring, the muon lifetime would be only 0.15 s, and the scheme would be considerably more challenging.

FUTURE STUDIES AND OPTIONS

Since the positron bunch will be mismatched to the non-linear plasma response, some filamentation and transverse emittance growth will result, perhaps by as much as two orders of magnitude. However, the initial positron geometric emittance from the booster can be extremely small (sub-nm horizontally and pm level vertically [2]). The resulting transverse emittance of the produced muons will need to be simulated and optimized, by adjusting positron beam parameters and the optical functions at the entrance to the plasma. As a next step, muon generation by e^+e^- annihilation in — and the subsequent muon transport through — the plasma will need to be included in these simulations. If the emittance of the muon beam emerging from the plasma target is small enough, subsequent plasma acceleration stages can be considered for rapidly increasing the muon beam energy.

Along the way, a phase rotation (bunch compression) of the muons may be required, since the initial bunch length of ~ 5 m, for the positrons or resulting muons, will still be too long for collider operation. While, in the scheme presented, no muon accumulation is foreseen, adding a 140 m accumulator ring, like the one designed for a thin target in Ref. [4], could allow sending, instead, multiple shorter positron bunches through the plasma.

ACKNOWLEDGEMENTS

We thank E. Gschwendtner and A. Pukhov for helpful discussions, and K. Lotov for support with LCODE.

REFERENCES

- [1] M. Antonelli, M. Boscolo, R. Di Nardo, and P. Raimondi, “Novel proposal for a low emittance muon beam using positron beam on target,” *Nucl. Instrum. Meth. A*, vol. 807, pp. 101–107, 2016, doi:10.1016/j.nima.2015.10.097
- [2] A. Abada, M. Abbrescia, S. S. AbdusSalam *et al.*, “FCC-ee: The Lepton Collider,” *Eur. Phys. J. Spec. Top.*, vol. 228, 2019, doi:10.1140/epjst/e2019-900045-4
- [3] F. Zimmermann, “LHC/FCC-based muon colliders,” *Journal of Physics: Conference Series*, vol. 1067, p. 022017, 2018, doi:10.1088/1742-6596/1067/2/022017
- [4] M. Boscolo, M. Antonelli, A. Ciarma, and P. Raimondi, “Muon production and accumulation from positrons on target,” *Phys. Rev. Accel. Beams*, vol. 23, p. 051001, 5 2020, doi:10.1103/PhysRevAccelBeams.23.051001
- [5] M. W. Krasny, “The Gamma Factory proposal for CERN,” arXiv 1511.07794, 2015.
- [6] K. Takayama *et al.*, “Induction acceleration of heavy ions in the KEK digital accelerator: Demonstration of a fast-cycling induction synchrotron,” *Phys. Rev. ST Accel. Beams*, vol. 17, no. 1, p. 010101, 2014, doi:10.1103/PhysRevSTAB.17.010101
- [7] J. Barraza *et al.*, “Upgrades to the DAHRT Second Axis Induction Cells,” *Conf. Proc. C*, vol. 070625, p. 2385, 2007, doi:10.1109/PAC.2007.4441258
- [8] K. Takayama and R. J. Briggs, Eds., *Induction Accelerators*. Springer, 2011, doi:10.1007/978-3-642-13917-8
- [9] BINP PWFA Team 2019, *LCODE Framework Description and Manual*, 2019, <https://lcode.info/>
- [10] K. V. Lotov, “Fine wakefield structure in the blowout regime of plasma wakefield accelerators,” *Phys. Rev. ST Accel. Beams*, vol. 6, p. 061301, 6 2003, doi:10.1103/PhysRevSTAB.6.061301
- [11] A. Sosedkin and K. Lotov, “LCODE: A parallel quasistatic code for computationally heavy problems of plasma wakefield acceleration,” *Nucl. Instr. Meth. Phys. Res. A*, vol. 829, pp. 350–352, 2016, doi:10.1016/j.nima.2015.12.032
- [12] J. M. Dawson, “Nonlinear electron oscillations in a cold plasma,” *Phys. Rev.*, vol. 113, pp. 383–387, 2 1959, doi:10.1103/PhysRev.113.383
- [13] E. Adli *et al.*, “Acceleration of electrons in the plasma wakefield of a proton bunch,” *Nature*, vol. 561, no. 7723, pp. 363–367, 2018, doi:10.1038/s41586-018-0485-4
- [14] A. A. Gorn *et al.*, “Proton beam defocusing in AWAKE: Comparison of simulations and measurements,” *Plasma Physics and Controlled Fusion*, vol. 62, no. 12, p. 125023, 2020, doi:10.1088/1361-6587/abc298
- [15] A. Latina, *RFTRACK Code Repository and Manual*, 2020, <https://gitlab.cern.ch/rf-track>
- [16] A. Latina, *Rf-track reference manual*, version 2.0.4, 2020, doi:10.5281/zenodo.3887085